AKT1-FOXO4 AXIS REGULATES HEMOCHORIAL PLACENTATION

Keisuke Kozai[1,*,§], Ayelen Moreno-Irusta[1,*], Khursheed Iqbal[1], Mae-Lan Winchester[2†], Regan L. Scott[1], Mikaela E. Simon[1], Masanaga Muto[1‡], Marc R. Parrish[2], and Michael J. Soares[1,2,3,¥]

[1]Institute for Reproduction and Perinatal Research, Department of Pathology & Laboratory Medicine, University of Kansas Medical Center, Kansas City, KS

[2]Department of Obstetrics and Gynecology, University of Kansas Medical Center, Kansas City, KS

[3]Center for Perinatal Research, Children's Mercy Research Institute, Children's Mercy, Kansas City, MO

***Contributed equally**

[¥]Correspondence: msoares@kumc.edu

[§]Present address: Department of Obstetrics and Gynecology, University of Missouri-Kansas City School of Medicine, Kansas City, MO

[†]Present address: Department of Obstetrics and Gynecology, University Hospital, Case Western Reserve University, Beachwood, OH 44122

[‡]Present address: Department of Stem Cells and Human Disease Models, Research Center for Animal Life Science, Shiga University of Medical Science, Seta, Tsukinowa-cho, Otsu, Shiga 520-2192, Japan

Running title:AKT1 and uteroplacental development

Keywords: AKT1, FOXO4, trophoblast, placenta, pregnancy, rat, genome editing

ABSTRACT

AKT1 is a serine/threonine kinase implicated in fetal, placental, and postnatal growth. In this study, we investigated roles for AKT1 in placental development using a genome-edited/loss-of-function rat model. Both heterozygous and homozygous *Akt1* mutant rats were viable and fertile. Disruption of AKT1 resulted in placental, fetal, and postnatal growth restriction. *Akt1* null placentas showed deficits in both junctional zone and labyrinth zone size. Robust differences in the transcriptome of wild type versus *Akt1* null junctional zones were identified. Forkhead box O4 (***Foxo4***), which encodes a transcription factor and known AKT substrate, was abundantly expressed in the junctional zone. FOXO4 expression was prominent in the junctional zone and invasive trophoblast cells of the rat placentation site and enhanced following rat trophoblast stem cell differentiation. *Foxo4* gene disruption using genome-editing resulted in placentomegaly, including an enlarged junctional zone. AKT1 and FOXO4 regulate the expression of many of the same transcripts expressed by trophoblast cells; however, in opposite directions. In summary, we have identified AKT1 and FOXO4 as part of a regulatory network controlling hemochorial placenta development.

INTRODUCTION

The placenta is an extraembryonic structure essential for normal fetal development (**Maltepe & Fisher, 2015; Burton *et al.*, 2016**). Placentas possess two main functions: i) transformation of the maternal environment to support viviparity and ii) regulation of the transfer of nutrients to the fetus (**Gardner & Beddington, 1988; Soares *et al.*, 2018; Knöfler *et al.*, 2019**). These specialized functions are ascribed to trophoblast cells, which differentiate along a multi-lineage pathway and are situated within specific compartments of the placenta (**Gardner & Beddington, 1988; Soares *et al.*, 2018; Knöfler *et al.*, 2019; Aplin & Jones, 2021**). Placentas come in different shapes, sizes, and connectivity to the mother (**Wooding & Burton, 2008; Roberts *et al.*, 2016**). Placentation in some mammalian species is characterized by trophoblast cells migrating into the maternal uterus where they modify the vasculature facilitating maternal nutrient flow to the placenta (**Pijnenborg *et al.*, 1981; Soares *et al.*, 2018**). This type of placenta is referred to as hemochorial (**Wooding & Burton, 2008; Roberts *et al.*, 2016**). The human and rat possess hemochorial placentation where invasive trophoblast cells migrate deep into the uterine parenchyma (**Pijnenborg *et al.*, 1981; Soares *et al.*, 2018**). Regulation of deep hemochorial placentation is poorly understood. The rat represents a useful animal model for investigating the regulation of deep hemochorial placentation (**Pijnenborg & Vercruysse, 2010; Soares *et al.*, 2012; Shukla & Soares, 2022**).

The rat placenta can be divided into two main compartments: i) junctional zone; ii) labyrinth zone (**Ain *et al.*, 2006; Soares *et al.*, 2012**). The junctional zone compartment of the placenta is situated proximal to the uterine endometrium and is responsible for transforming the maternal environment, whereas the labyrinth zone is located between the junctional zone and fetus where it facilitates nutrient delivery to the fetus (**Knipp *et al.*,**

1999; Soares *et al.*, 2012). Junctional zone-specific functions include the production of peptide and steroid hormones that target maternal organs and the generation of invasive trophoblast cells that migrate into and restructure the uterine parenchyma (**Soares *et al.*, 1996, 2012**). The extravillous trophoblast cell column is a structure within the human placentation site, which shares some of these same responsibilities (**Soares *et al.*, 2018; Knöfler *et al.*, 2019**). The junctional zone and extravillous trophoblast cell column are pivotal to the regulation of maternal adaptations to pregnancy, yet little is known about how they are regulated.

In this report, we focus on the phosphatidylinositol 3-kinase (**PI3K**)/AKT pathway and its involvement in regulating junctional zone biology. AKT1 is one of three AKT serine/threonine kinases and represents an integral component of signal transduction pathways regulating cell proliferation, differentiation, migration, survival, and metabolism (**Manning & Toker, 2017; Cole *et al.*, 2019**). AKT1 has also been implicated in placentation and trophoblast cell development through rodent mutagenesis experiments and investigations with human trophoblast cells (**Kamei *et al.*, 2002; Yang *et al.*, 2003; Qiu *et al.*, 2004; Dash *et al.*, 2005; Kent *et al.*, 2010, 2011, 2012; Plaks *et al.*, 2011; Haslinger *et al.*, 2013; Sharma *et al.*, 2016**). Disruptions in AKT signaling have been connected to trophoblast cell dysfunction leading to recurrent pregnancy loss, preeclampsia, and infertility (**Pollheimer & Knöfler, 2005; Ferretti *et al.*, 2007; Fisher, 2015; Burton & Jauniaux, 2018**). Herein we show that AKT1 inactivation leads to placental and fetal growth restriction in the rat. AKT1 acts via phosphorylation of its target proteins leading to functional changes, including activation or inhibition of the target protein function (**Manning & Toker, 2017; Cole *et al.*, 2019**). We identified forkhead box O4 (**FOXO4**), a transcription factor, as an AKT1 substrate within the rat junctional zone and in rat trophoblast cells and demonstrated FOXO4

involvement in junctional zone development and the regulation of trophoblast cell differentiation.

RESULTS

Generation of an *Akt1* mutant rat model

We examined the role of AKT1 in regulating deep placentation in the rat using CRISPR/Cas9 genome editing. A mutant rat strain possessing a 1,332 bp deletion within the *Akt1* gene was generated (**Fig. 1A and B**). The deletion included part of Exon 4, the entire region spanning Exon 5 through Exon 6, and part of Exon 7 and led to a frameshift and premature stop codon (**Fig. 1A and B**). The deletion effectively removed the kinase domain and regulatory regions of AKT1 (**Fig. 1C**). The *Akt1* mutation was successfully transmitted through the germline. A rat colony possessing the *Akt1* mutation was established and maintained via heterozygous x heterozygous breeding. Mating of heterozygotes produced the predicted Mendelian ratio (**Fig. 1D; Supplemental Table 1**). Placental tissues possessing a homozygous deletion within the *Akt1* locus (*Akt1*$^{-/-}$) were deficient in AKT1 protein and exhibited prominent deficits in pan-AKT and phospho-AKT protein expression (**Fig. 1E**). These findings support the successful disruption of the *Akt1* locus and are consistent with AKT1 being the predominant AKT isoform within the placenta (**Yang *et al.*, 2003; Kent *et al.*, 2011; Haslinger *et al.*, 2013**).

AKT1 deficiency results in placental, fetal, and postnatal growth restriction

Disruption of the *Akt1* locus in the mouse disrupts placental, fetal, and postnatal growth (**Chen *et al.*, 2001; Cho *et al.*, 2001; Yang *et al.*, 2003; Plaks *et al.*, 2011; Kent et al., 2012**). We observed a similar phenotype in the rat. Gestation day (**gd**) 18.5 placental and fetal weights and postnatal pup weights were significantly smaller in the *Akt1*$^{-/-}$ rat model when

compared to *Akt1*$^{+/+}$ rats (**Fig. 2A-H**). Junctional and labyrinth zone compartments of the placenta were also significantly smaller in *Akt1*$^{-/-}$ placentas (**Fig. 2D, E, I**).

AKT1 regulates junctional zone and invasive trophoblast cell phenotypes

Transcript profiles were determined for *Akt1*$^{+/+}$ and *Akt1*$^{-/-}$ gd 18.5 junctional zone tissues using RNA-sequencing (**RNA-seq**). The size and morphological phenotypes associated with inactivation of AKT1 were associated with distinct transcript profiles (**Fig. 3; Dataset 1**). Disruption of AKT1 resulted in upregulation of 254 transcripts and downregulation of 333 transcripts (**Dataset 1**). Pathway analysis included signatures for cell cycle, DNA replication, cellular senescence, and PI3K-AKT signaling pathways (**Fig. 3A**). Transcripts encoding cell cycle progression were consistently repressed in the *Akt1*$^{-/-}$ junctional zones (**Fig. 3A and B**). In addition, we also observed prominent downregulation of a member of the expanded prolactin (**PRL**) gene family, *Prl8a4*, and the upregulation of cellular communication network factor 3 (*Ccn3*, also called *Nov*; **Fig. 3B**).

The junctional zone serves as the source of invasive trophoblast cells entering the uterus. Consequently, we investigated the uterine-placental interface of *Akt1*$^{+/+}$ and *Akt1*$^{-/-}$ placentas and monitored the surface area occupied by intrauterine invasive trophoblast cells and the expression of invasive trophoblast cell-specific transcripts. *Akt1*$^{-/-}$ invasive trophoblast cells exhibited decreased infiltration into the uterus (**Supplemental Fig. 1A-C**). We also observed approximately a 50% decrease in the expression of cytokeratin transcripts, which are typically expressed by invasive trophoblast cells within the uterine-placental interface (**Supplemental Fig. 1D**). More prominent decreases in expression of invasive trophoblast-cell specific transcripts were observed in uterine-placental interface tissue associated with *Akt1*$^{-/-}$ placentas (**Supplemental Fig. 1D**).

Collectively, the data indicate that AKT1 signaling has profound effects on development of the junctional zone and the invasive trophoblast cell lineage.

FOXO4 is a target of PI3K/AKT signaling

Forkhead box (**FOX**) transcription factors are known targets of PI3K/AKT signaling and have key roles in regulating developmental processes (**Lam *et al.*, 2013; Schmitt-Ney, 2020; Herman *et al.*, 2021**). We interrogated RNA-seq datasets from wild type gd 18.5 junctional zone for FOX family transcription factors. Transcripts for several FOX transcription factors were detected (transcripts per million, TPM value ≥ 1.0) (**Fig. 4A**). *Foxo4* transcripts were striking in their abundance relative to all other FOX family members. AKT1 did not significantly affect expression levels for any of the FOX family transcripts (**Dataset 1**). *Foxo4* transcripts were specifically localized to the junctional zone and a subset of invasive trophoblast cells localized to uterine spiral arteries, termed endovascular invasive trophoblast cells (**Fig. 4B and C**). Total and phosphorylated FOXO4 protein were significantly diminished in *Akt1* null junctional zones (**Fig. 4D**). We next explored FOXO4 in differentiated rat trophoblast stem (**TS**) cells, a model for trophoblast cell lineages found in the junctional zone (**Asanoma *et al.*, 2011**). *Foxo4* transcript and total and phosphorylated FOXO4 protein showed striking increases in abundance following TS cell differentiation (**Fig. 4E-F**). As previously demonstrated, AKT activity increased following trophoblast cell differentiation (**Kamei *et al.*, 2002; Kent *et al.*, 2010, 2011; Fig. 4G**). AKT activation was required for optimal FOXO4 phosphorylation (**Fig. 4G**). Thus, we established a link between PI3K/AKT signaling and FOXO4 in trophoblast cell lineage development.

Generation of a *Foxo4* mutant rat model

We examined the role of FOXO4 in regulating placentation in the rat using CRISPR/Cas9 genome editing. The *Foxo4* gene consists of four exons and resides on the X chromosome (**Liu *et al.*, 2020**). A mutant rat strain possessing a 3,096 bp deletion within the *Foxo4* gene was generated (**Fig. 5A and B**). The deletion included the 3' part of Exon 2 and the 5' part of Exon 3 and led to a frameshift and a premature stop codon (**Fig. 5A and B**). The deletion effectively disrupted the conserved forkhead DNA binding domain and removed nuclear localization, nuclear export, and transactivation domains of FOXO4 (**Fig. 5C**). The *Foxo4* mutation was successfully transmitted through the germline (**Fig. 5D; Supplemental Table 2**). A rat colony possessing the *Foxo4* mutation was established and maintained via hemizygous male x wild type female breeding, which produced the predicted Mendelian ratio (**Supplemental Table 2**). Junctional zone tissues possessing a maternally inherited *Foxo4* mutation ($Foxo4^{Xm-}$) were deficient in FOXO4 protein (**Fig. 5E**). The results are consistent with paternal silencing of X chromosome-linked genes expressed in extraembryonic tissues (**Takagi & Sasaki, 1975; West et al., 1978; Hemberger, 2002**). FOXO4 was successfully disrupted in the rat.

FOXO4 deficiency results in placentomegaly and a modified junctional zone phenotype

Placentation site phenotypes of mice possessing mutations at the *Foxo4* locus have not been described (**Liu *et al.*, 2020; Hosaka *et al.*, 2004**). Rats possessing a maternally inherited mutant *Foxo4* allele ($Foxo4^{Xm-}$) exhibited placentomegaly and decreased placental efficiency (fetal/placental weight ratio) when examined on gd 18.5 (**Fig. 6A-C**) and gd 20.5 (**Supplemental Fig. 2A-C**). In contrast, a paternally inherited mutant *Foxo4* allele did not significantly affect placenta or fetal weights (**Supplemental Fig. 2D and E**). FOXO4 deficiency associated placentomegaly included significantly larger junctional and labyrinth zones (**Fig. 6D-G, Supplemental Fig. 2F-H**) but did not affect the intrauterine invasive

trophoblast cell lineage (**Supplemental Fig. 3**). Transcript profiles were determined for wild type (*Foxo4*$^{Xm+}$) and *Foxo4*$^{Xm-}$ gd 18.5 junctional zone tissues using RNA-seq (**Fig. 6H**). Disruption of FOXO4 resulted in upregulation of 369 transcripts and downregulation of 845 transcripts (**Dataset 2**). Pathway analysis included signatures for PI3K-AKT signaling, cell cycle, DNA replication, extracellular matrix receptor interaction, and complement and coagulation pathways (**Fig. 6H**). Junctional adhesion molecule-like (**JAML**), lipoprotein(a) like 2 (**LPAL2**), erb-b2 receptor tyrosine kinase 3 (**ERBB3**), and growth factor receptor bound protein 7 (**GRB7**) were each conspicuous in their prominent downregulation in FOXO4 deficient junctional zone tissue (**Fig. 6I**). JAML contributes to epithelial barrier function, modulates immune cell trafficking, and angiogenesis (**Kummer & Ebnet, 2018**), whereas LPAL2 is a long noncoding RNA contributing to inflammatory and oxidative stress responses (**Han *et al.*, 2018**). JAML and LPAL2 have not previously been linked to trophoblast or placental biology. ERBB3 is a receptor for neuregulin 1 and promotes trophoblast cell survival (**Fock *et al.*, 2015**) and GRB7 is an adaptor protein participating in signal transduction activated through ERBB3 (**Fiddes *et al.*, 1998**). Interestingly, numerous junctional zone transcripts regulated by FOXO4 were reciprocally regulated by AKT1 (88% of transcripts upregulated in *Akt1* null were downregulated in *Foxo4* mutant tissues; 38% of transcripts downregulated in *Akt1* null were upregulated in *Foxo4* mutant tissues; **Fig. 7**). The reciprocal relationship between AKT1 and FOXO4 is evident at structural and molecular levels.

FOXO4 contributes to the regulation of the trophoblast cell lineage

We next modeled junctional zone cell biology using rat TS cells. The consequences of FOXO4 disruption in differentiating rat TS cells were examined. FOXO4 expression was inhibited via ectopic expression of short hairpin RNAs specific to *Foxo4* (**Fig. 8A and B**).

Although, a morphologic phenotype was not evident, prominent differences in the transcriptomes of TS cells expressing control versus *Foxo4* shRNAs were observed (**Fig. 8C**). Disruption of FOXO4 resulted in upregulation of 260 transcripts and downregulation of 443 transcripts (**Dataset 3**). Pathway analysis included signatures for PI3K-AKT signaling, longevity regulating, calcium signaling, and glutathione metabolism pathways (**Fig. 8C**). Among the dysregulated transcripts was an upregulation of matrix metallopeptidase 12, a known constituent of endovascular invasive trophoblast cells (**Harris et al., 2010; Chakraborty et al., 2016**) and downregulation of trophoblast specific protein alpha, a transcript characteristic of spongiotrophoblast cells within the junctional zone (**Iwatsuki *et al.*, 2000**). FOXO4 is a known regulator of responses to oxidative stress (**Liu *et al.*, 2020**). Several transcripts associated with inflammatory and cellular stress responses, including thioredoxin interacting protein, glutathoione S-transferase mu 1, arachidonate 5-lipoxygenase activating protein, interferon kappa, nuclear protein 1, and *Lpal2*, were prominently downregulated (**Sies & Cadenas, 1985; LaFleur *et al.*, 2001; Mashima & Okuyama, 2015; Han *et al.*, 2018; Huang *et al.*, 2021; Nirgude & Choudhary, 2021; Qayyum *et al.*, 2021; Satapathy & Wilson, 2021**).

Key findings

Collectively, the results indicate that AKT1 drives placental growth, including regulation of deep intrauterine trophoblast cell invasion. These actions are accomplished, at least in part, through modulation of FOXO4, which acts to restrain placental growth and coordinate responses to physiological stressors.

DISCUSSION

The rat and human possess a type of hemochorial placentation where specialized trophoblast cells penetrate deep into the uterus and transform the uterine parenchyma, including the vasculature (**Pijnenborg *et al.*, 1981; Pijnenborg & Vercruysse, 2010; Soares *et al.*, 2012**). Central to deep placentation is the source of invasive trophoblast cells, which in the rat is a compartment within the placenta referred as the junctional zone and, in the human, the extravillous trophoblast cell column (**Soares *et al.*, 2012, 2018; Knöfler *et al.*, 2019**). In addition to an intrauterine role, the cellular constituents of these placental compartments produce hormones directed to maternal tissues with actions that ensure in utero survival and promotion of fetal growth (**Soares *et al.*, 1996; John, 2017**). In this report, AKT1 and FOXO4 were identified as regulators of rat junctional zone development. In vivo disruption of AKT1 and FOXO4 led to opposite effects on junctional zone development. AKT1 deficiency resulted in growth restriction of the junctional zone, phenotypic alteration of the invasive trophoblast cell lineage, as well as compromised fetal and postnatal growth, and AKT1 was capable of phosphorylating FOXO4 in rat trophoblast cells. Deficiency of FOXO4 resulted in an expanded junctional zone. Deficits in AKT1 or FOXO4 also impacted transcriptomic profiles of the junctional zone. The findings indicate that AKT1 and FOXO4 are part of a gene regulatory network controlling hemochorial placentation.

AKT1 signaling influenced placental development. *Akt1* null mutations in the mouse and rat yield similar phenotypes characterized by placental, fetal, and postnatal growth restriction (**Chen *et al.*, 2001; Cho *et al.*, 2001; Yang *et al.*, 2003; Plaks *et al.*, 2011; Kent et al., 2012**). Smaller junctional zones accompanying AKT1 deficiency were associated with a downregulation of transcripts encoding proteins driving cell proliferation. These results imply that size differences of junctional zone compartments in the wild type versus *Akt1* nulls were

related to, at least in part, diminished trophoblast cell proliferation in *Akt1* junctional zone tissues. The data also fit well with known actions of AKT signaling promoting cell proliferation in a wide range of cell types (**Manning & Cantley, 2007; Manning & Toker, 2017; Cole *et al.*, 2019**). AKT1 disruption also altered differentiated junctional zone trophoblast cell phenotypes. As cellular constituents of the junctional zone differentiate, they acquire the capacity to express several members of the expanded prolactin (**PRL**) family of hormones/cytokines (**Soares, 2004; Alam *et al.*, 2006; Soares *et al.*, 2007**). The expression of PRL8A4, a member of the expanded PRL family, was dramatically downregulated in *Akt1* null junctional zones. PRL8A4 is an orphan ligand with little known of its significance to the biology of pregnancy other than as a signature feature of the differentiated junctional zone phenotype (**Iwatsuki *et al.*, 1998; Soares *et al.*, 2007**). AKT signaling has previously been implicated in the regulation of the differentiation of rodent and human trophoblast cells (**Kamei *et al.*, 2003; Kent *et al.*, 2010, 2011; Haslinger *et al.*, 2013**). Disruption of *Akt1* also interfered with invasive trophoblast cell development. Trophoblast cell infiltration into the uterine-placental interface was diminished in *Akt1* nulls as was the expression of transcripts indicative of the invasive trophoblast cell lineage. Involvement of AKT signaling has also been implicated in the development of the human extravillous trophoblast cell lineage (**Pollheimer & Knöfler, 2005; Haslinger *et al.*, 2013; Morey *et al.*, 2021**). AKT signaling could affect invasive trophoblast cell development through its actions on their origin in the junctional zone and EVT cell column or alternatively, their maturation as they invade into the uterus. Finally, the impact of AKT signaling in invasive trophoblast cell development may be more profound than observed with AKT1 deficiency due to compensatory activities of AKT2 and AKT3 (**Kent *et al.*, 2011; Haslinger *et al.*, 2013**).

AKT1 regulates cellular function through its actions as a serine/threonine kinase and thus, phosphorylation of its substrates (**Manning & Cantley, 2007; Manning & Toker, 2017; Cole *et al.*, 2019**). The forkhead box (**FOX**) family of transcription factors are well-established targets of AKT action (**Lam *et al.*, 2013; Schmitt-Ney, 2020; Herman *et al.*, 2021**). Among FOX family members, FOXO4 expression was uniquely elevated in the rat junctional zone. FOXO4 phosphorylation state in trophoblast cells was affected by AKT signaling. AKT-mediated phosphorylation of FOXO4 leads to FOXO4 exit from the nucleus and inactivation (**Schmitt-Ney, 2020; Herman *et al.*, 2021**), which might suggest that an AKT1 deficiency would result in the stabilization of FOXO4 protein in the junctional zone. Instead, AKT1 deficiency led to depletion of junctional zone total and phosphorylated FOXO4 proteins. Consequently, the observed *Akt1* null placental phenotype was associated with the depletion of both AKT1 and FOXO4 proteins. In addition to regulation by AKT signaling, FOXO4 activity/stability is stimulated by Jun kinase and monoubiquitylation (**Essers *et al.*, 2004; van der Horst *et al.*, 2006; Brenkman *et al.*, 2008; Liu *et al.*, 2020**), while inhibited by acetylation and polyubiquitylation (**Fukuoka *et al.*, 2003; Huang & Tindall, 2011; Liu *et al.*, 2020**). Whether AKT1 indirectly affects FOXO4 protein via impacting these other FOXO4 regulators remains to be determined.

FOXO4 is a transcription factor implicated in the regulation of the cell cycle, apoptosis, responses to oxidative stress, and a range of disease processes (**Liu *et al.*, 2020**). The original characterization of the *Foxo4* null mouse concluded that FOXO4 did not have a singular role in the pathophysiology of the mouse (**Hosaka *et al.*, 2004**). The absence of a reported phenotype for the *Foxo4* null mouse model was attributed to the compensatory actions of other members of the FOXO family, including FOXO1, FOXO3, and possibly FOXO6 (**Hosaka *et al.*, 2004; Liu *et al.*, 2020**). We describe a prominent placental phenotype for the

Foxo4 null rat model. The placental anomalies associated with FOXO4 deficiency were compatible with the production of viable offspring. The absence of a fertility defect in the *Foxo4* null mouse model likely precluded a closer examination of placentation (**Hosaka *et al.*, 2004**). However, it is also possible that elements of FOXO4 action are species specific. FOXO4 is prominently expressed in the junctional zone and to a lesser extent in invasive trophoblast cells. Disruption of FOXO4 led to an expansion of both junctional and labyrinth zone placental compartments, which probably reflects cell autonomous and non-cell autonomous actions, respectively. A striking reciprocal pattern of AKT1 versus FOXO4 gene regulation within the junctional zone was demonstrated and included differentially regulated transcripts encoding proteins involved in the regulation of cell proliferation and cell death. We surmise that AKT1 promotes junctional zone growth via stimulating the expression of transcripts connected to cell cycle progression and inhibited transcripts connected to cell death, whereas the converse is true for FOXO4. These biological roles are consistent with the known actions of AKT1 and FOXO4 in other cell systems (**Manning & Toker, 2017; Liu *et al.*, 2020; Herman *et al.*, 2021**). A transcriptional regulatory network involving FOXO4 has also been identified in human extravillous trophoblast cells (**Morey *et al.*, 2021**). Importantly, FOXO4 also regulates trophoblast cell responses to oxidative stress and is thus, positioned to contribute to placental adaptations to a compromised maternal environment and in disease states affecting placentation.

MATERIALS AND METHODS

Animals

Holtzman Sprague-Dawley rats were maintained in an environmentally controlled facility with lights on from 0600 to 2000 h with food and water available ad libitum. Time-mated pregnancies were established by co-housing adult female rats (8-10 weeks of age) with adult

male rats (>10 weeks of age). Detection of sperm or a seminal plug in the vagina was designated gd 0.5. Pseudopregnant females were generated by co-housing adult female rats (8-10 weeks of age) with adult male vasectomized males (>10 weeks of age). The detection of seminal plugs was designated pseudopregnancy day 0.5. Four to five-week-old donor rats were superovulated by intraperitoneal injection of pregnant mare serum gonadotropin (30 units, G4877, Sigma-Aldrich, St. Louis, MO), followed by an intraperitoneal injection of human chorionic gonadotropin (30 units, C1063, Sigma-Aldrich) ~46 h later, and immediately mated with adult males. Zygotes were flushed from oviducts the next morning (gd 0.5). The University of Kansas Medical Center (**KUMC**) Animal Care and Use Committee approved all protocols involving the use of rats.

Tissue collection and analysis

Rats were euthanized by CO_2 asphyxiation at designated days of gestation. Uterine segments containing placentation sites were frozen in dry ice-cooled heptane and stored at -80ºC until processed for histological analyses. Alternatively, placentation sites were dissected into placentas, the adjacent uterine-placental interface tissue (also referred to as the metrial gland), and fetuses as previously described (**Ain *et al.*, 2006**). Placentas were weighed and dissected into junctional zone and labyrinth zone compartments (**Ain *et al.*, 2006**). Placental compartments and uterine-placental interfaces were frozen in liquid nitrogen and stored at -80ºC until used for biochemical analyses. Fetuses were weighed, genotyped, and sex determined by polymerase chain reaction (**PCR**) (**Dhakal & Soares, 2017**).

Generation of *Akt1* and *Foxo4* mutant rat models

Mutations at *Akt1* and *Foxo4* loci were generated using CRISPR/Cas9 genome editing (**Kaneko, 2017; Iqbal *et al.*, 2021**). Guide RNAs targeting Exon 4 (target sequence:

GCCGTTTGAGTCCATCAGCC; nucleotides 356-375) and Exon 7 (target sequence: TTGTCATGGAGTACGCCAAT; nucleotides 712-731) of the *Akt1* gene (NM_033230.3) or targeting Exon 2 (target sequence: CCAGATATACGAATGGATGGTCC; nucleotides 517-539) and Exon 3 (target sequence: GTTCATCAAGGTACATAACGAGG; nucleotides 631-653) of the *Foxo4* gene (NM_001106943.1) were electroporated into single-cell rat embryos using the NEPA21 electroporator (Nepa Gene Co Ltd, Ichikawa City, Japan). Electroporated embryos were transferred to oviducts of day 0.5 pseudopregnant rats. Initially, offspring were screened for *Akt1* or *Foxo4* mutations from genomic DNA from tail-tip biopsies using the REDExtract-N-Amp^{TM} Tissue PCR kit (XNAT, Millipore Sigma, Burlington, MA). PCR was performed on the purified DNA samples using primers flanking the guide RNA sites, and products resolved by agarose gel electrophoresis and ethidium bromide staining. Genomic DNA containing potential mutations was amplified by PCR, gel purified, and precise boundaries of deletions determined by DNA sequencing (Genewiz Inc., South Plainfield, NJ). Founders with *Akt1* or *Foxo4* mutations were backcrossed to wild type rats to demonstrate germline transmission. Routine genotyping was performed by PCR on genomic DNA with specific sets of primers (**Supplemental Table 3**).

Western blot analysis

Tissue lysates were prepared with radioimmunoprecipitation assay lysis buffer system (sc-24948A, Santa Cruz Biotechnology, Santa Cruz, CA). Protein concentrations were determined using the *DC*^{TM} Protein Assay Kit (5000112, Bio-Rad Laboratories, Hercules, CA). Proteins (20 µg/lane) were separated by SDS-PAGE. Separated proteins were electrophoretically transferred to polyvinylidene difluoride membranes (10600023, GE Healthcare, Milwaukee, WI) for 1 h at 100 V on ice. Membranes were subsequently blocked with 5% milk or 5% bovine serum albumin for 1 h at room temperature and probed separately

with specific primary antibodies to AKT1 (1:1,000 dilution, 75692, Cell Signaling Technology, Danvers, MA), pan-AKT (1:1,000 dilution, 4691, Cell Signaling Technology), phospho-Ser^{473} AKT (1:2,000 dilution, 4060, Cell Signaling Technology), FOXO4 (1:2,000 dilution, 21535-1-AP, Proteintech, Rosemont, IL), phospho-Ser^{262} FOXO4 (1:3,000 dilution, ab126594, Abcam, Cambridge, MA), and glyceraldehyde 3-phosphate dehydrogenase (**GAPDH**, 1:5,000 dilution, ab8245, Abcam) in Tris-buffered saline with Tween 20 (**TBST**) overnight at 4□. After primary antibody incubation, the membranes were washed in TBST three times for ten min each at room temperature. After washing, the membranes were incubated with anti-rabbit or anti-mouse immunoglobulin G (**IgG**) conjugated to horseradish peroxidase [**HRP**, 1:5,000 dilution or 1:20,000 dilution (phospho-Ser^{262} FOXO4), 7074S and 7076S, Cell Signaling Technology] in TBST for 1 h at room temperature, washed in TBST three times for ten min each at room temperature, immersed in Immobilon Crescendo Western HRP Substrate (WBLUR0500, Sigma-Aldrich), and luminescence detected using Radiomat LS film (Agfa Healthcare, Mortsel, Belgium).

Transcript analysis

Total RNA was extracted from tissues using TRI Reagent Solution (AM9738, Thermo-Fisher, Waltham, MA) according to the manufacturer's instructions. Total RNA (1 μg) was reverse transcribed using a High-Capacity cDNA Reverse Transcription Kit (4368813, Thermo-Fisher). Complementary DNAs were diluted 1:10 and subjected to reverse transcription-quantitative PCR (**RT-qPCR**) using PowerUp SYBR Green Master Mix (A25742, Thermo-Fisher) and primers provided in **Supplemental Table 4**. QuantStudio 5 Flex Real-Time PCR System (Applied Biosystems, Foster City, CA) was used for amplification and fluorescence detection. PCR was performed under the following conditions: 95□ for 10 min, followed by 40 cycles of 95□ for 15 sec and 60□ for 1 min.

Relative mRNA expression was calculated using the delta-delta Ct method. *Gapdh* was used as a reference transcript.

RNA-seq analysis

Transcript profiles were generated from wild type and *Akt1*$^{-/-}$, and *Foxo4*$^{Xm-}$ junctional zone tissues, and rat differentiated TS cells expressing control or *Foxo4* shRNAs. Complementary DNA libraries from total RNA samples were prepared with Illumina TruSeq RNA preparation kits according to the manufacturer's instructions (Illumina, San Diego, CA). RNA integrity was assessed using an Agilent 2100 Bioanalyzer (Santa Clara, CA). Barcoded cDNA libraries were multiplexed onto a TruSeq paired-end flow cell and sequenced (100-bp paired-end reads) with a TruSeq 200-cycle SBS kit (Illumina). Samples were run on an Illumina NovaSeq 6000 sequencer at the KUMC Genome Sequencing Facility. Reads from *.fastq files were mapped to the rat reference genome (Ensembl Rnor_5.0.78) using CLC Genomics Workbench 12.0 (Qiagen, Germantown, MD). Transcript abundance was expressed as transcript per million mapped reads (TPM) and a *P* value of 0.05 was used as a cutoff for significant differential expression. Statistical significance was calculated by empirical analysis of digital gene expression followed by Bonferroni's correction. Pathway analysis was performed using Datbase for Annotation, Visualization, and Integrated Discovery (**DAVID; Huang *et al.*, 2009**).

Immunohistochemistry

Placentation sites were embedded in optimum cutting temperature (**OCT**) compound and sectioned at 10 μm thickness. Sections were fixed in 4% paraformaldehyde, washed in phosphate buffered saline (pH 7.4) three times for five min each, blocked with 10% normal goat serum (50062Z, Thermo-Fisher), and incubated overnight with primary antibodies: pan

cytokeratin (1:300 dilution, F3418, Sigma-Aldrich) to identify trophoblast cells and vimentin (1:300 dilution, sc-6260, Santa Cruz Biotechnology) to distinguish placental compartments. After washing with phosphate buffered saline (pH 7.4), sections were incubated with corresponding secondary antibodies: Alexa 568-conjugated goat anti-rabbit IgG (1:500 dilution, A11011, Thermo-Fisher) or rabbit anti-mouse IgG conjugated to HRP (1:500 dilution, A9044, Sigma-Aldrich) for 3 h at room temperature and color development with a 3-amino-9-ethylcarbazole (**AEC**) substrate kit (SK-4200, Vector Laboratories). Sections were then mounted with Fluoromount-G mounting media (0100-01, Southern Biotech, Birmingham, AL) and examined microscopically. Fluorescence images were captured on a Nikon 80i upright microscope (Nikon) with a Photometrics CoolSNAP-ES monochrome camera (Roper). The area occupied by cytokeratin-positive cells (invasive trophoblast cells) within the uterine-placental interface was quantified using ImageJ software, as previously described (**Nteeba *et al.*, 2020**).

In situ hybridization

Distributions of transcripts for *Foxo4* and *Prl7b1* were determined on cryosections of rat placentation sites. RNAscope Multiplex Fluorescent Reagent Kit version 2 (Advanced Cell Diagnostics, Newark, CA) was used for in situ hybridization analysis. Probes were prepared to detect *Foxo4* (NM_001106943.1, 1038981-C1, target region: 750-1651) and *Prl7b1* (NM_153738.1, 860181-C2, target region: 28-900). Fluorescence images were captured on a Nikon 80i upright microscope (Nikon) with a Photometrics CoolSNAP-ES monochrome camera (Roper).

Rat TS cell culture

Blastocyst-derived rat TS cells (**Asanoma *et al.*, 2011**) were cultured in Rat TS Cell

Medium [RPMI 1640 medium (11875093, Thermo-Fisher), 20% (vol/vol) fetal bovine serum (**FBS**, Thermo-Fisher), 100 µM 2-mercaptoethanol (M7522, Sigma-Aldrich), 1 mM sodium pyruvate (11360-070, Thermo-Fisher), 100 µM penicillin and 50 U/mL streptomycin (15140122, Thermo-Fisher)] supplemented with 70% rat embryonic fibroblast (REF)-conditioned medium prepared as described previously (Asanoma *et al*., 2011), 25 ng/ml fibroblast growth factor 4 (**FGF4**; 100-31, Peprotech), and 1 µg/mL heparin (H3149, Sigma-Aldrich). For induction of differentiation, rat TS cells were cultured for 15 days in rat TS medium containing 1% (vol/vol) FBS without FGF4, heparin, and REF-conditioned medium. In some experiments, rat TS cells were exposed to a phosphatidylinositol 3-kinase (**PI3K**) inhibitor (LY294002, 10 µM, 9901, Cell Signaling Technology).

Lentivirus construction and production

Lentivirus construction and production were described previously (**Muto *et al*., 2021; Varberg et al., 2021**). Briefly, the lentivirus encoding the shRNA targeting *Foxo4* (**Supplemental Table 5**) was constructed using a pLKO.1 vector. shRNA oligo sequences used in the analyses are provided in Supplemental Table 8. Lentiviral packaging vectors were obtained from Addgene and included pMDLg/pRRE (plasmid 12251), pRSV-Rev (plasmid 12253), pMD2.G (plasmid 12259). Lentiviral particles were produced using Attractene (301005, Qiagen) in human embryonic kidney (HEK) 293FT (Thermo-Fisher) cells.

Lentiviral transduction

Rat TS cells were incubated with lentiviral particles for 24 h followed by selection with puromycin dihydrochloride (5 µg/mL; A11138-03, Thermo-Fisher) for two days. Cells were then cultured for 1-3 days in Rat TS Cell Medium prior to differentiation.

Statistical analysis

Student's *t*-test, Welch's *t*-test, Dunnett's test, or Steel test were performed, where appropriate, to evaluate the significance of the experimental manipulations. Results were deemed statistically significant when $P < 0.05$.

ACKNOWLEDGEMENTS

The research was supported by postdoctoral fellowships from the Kansas Idea Network of Biomedical Research Excellence, P20 GM103418 (A.M-I.), Lalor Foundation (K.K., A.M-I., M.M.), American Heart Association (K.K., M.M.), and an NIH National Research Service Award, HD104495 (R.L.S.) and NIH grants (HD020676, HD079363, HD099638, HD105734), and the Sosland Foundation. We also thank Stacy Oxley and Brandi Miller for administrative assistance.

AUTHOR CONTRIBUTIONS

K.K., A.M.-I., and M.J.S. conceived and designed the research; K.K., A.M.-I., K.I., M.-L.W., R.L.S., M.E.S., M.M. performed experiments; K.K., A.M.-I., K.I., M.R.P., and M.J.S. analyzed the data and interpreted results of experiments; K.K., A.M.-I., and M.J.S. prepared figures and manuscript; All authors read, contributed to editing, and approved the final version of manuscript.

CONFLICT OF INTEREST

There is no conflict of interest that could be perceived as prejudicing the impartiality of the research reported.

DATA AVAILABILITY

RNA-seq datasets are available at the Gene Expression Omnibus (**GEO**) database, https://www.ncbi.nlm.nih.gov/geo/ (accession number GSE205831). All data generated and analyzed in this study are included in the published article and supporting files. Resources generated from the research are available from the corresponding author upon reasonable request. AKT1 and FOXO4 mutant rat models are available through the Rat Resource and Research Center (Columbia, MO).

REFERENCES

Ain R, Konno T, Canham LN, Soares MJ (2006) Phenotypic analysis of the rat placenta. *Methods Mol Med* 121: 295-313

Alam SM, Ain R, Konno T, Ho-Chen JK, Soares MJ (2006) The rat prolactin gene family locus: species-specific gene family expansion. *Mamm Genome* 17: 858-877

Aplin JD, Jones CJP (2021) Cell dynamics in human villous trophoblast. *Hum Reprod Update* 27: 904-922

Asanoma K, Rumi MA, Kent LN, Chakraborty D, Renaud SJ, Wake N, Lee DS, Kubota K, Soares MJ (2011) FGF4-dependent stem cells derived from rat blastocysts differentiate along the trophoblast lineage. *Dev Biol* 351: 110-119

Brenkman AB, de Keizer PL, van den Broek NJ, Jochemsen AG, Burgering BM (2008) Mdm2 induces mono-ubiquitination of FOXO4. *PLoS One* 3: e2819

Burton GJ, Fowden AL, Thornburg KL (2016) Placental origins of chronic disease. *Physiol*

549 *Rev* 96: 1509-1565

550

551 Burton GJ, Jauniaux E (2018) Pathophysiology of placental-derived fetal growth restriction.
552 *Am J Obstet Gynecol* 218(Suppl): S745-S761

553

554 Chakraborty D, Cui W, Rosario GX, Scott RL, Dhakal P, Renaud SJ, Tachibana M, Rumi MA,
555 Mason CW, Krieg AJ, Soares MJ (2016) HIF-KDM3A-MMP12 regulatory circuit ensures
556 trophoblast plasticity and placental adaptations to hypoxia. *Proc Natl Acad Sci USA* 113:
557 E7212-E7221

558

559 Chen WS, Xu PZ, Gottlob K, Chen ML, Sokol K, Shiyanova T, Roninson I, Weng W, Suzuki R,
560 Tobe K, et al. (2001) Growth retardation and increased apoptosis in mice with homozygous
561 disruption of the Akt1 gene. *Genes Dev* 15: 2203-2208

562

563 Cho H, Thorvaldsen JL, Chu Q, Feng F, Birnbaum MJ (2001) Akt1/PKBalpha is required for
564 normal growth but dispensable for maintenance of glucose homeostasis in mice. *J Biol Chem*
565 276: 38349-38352

566

567 Cole PA, Chu N, Salguero AL, Bae H (2019) AKTivation mechanisms. *Curr Opin Struct Biol*
568 59: 47-53

569

570 Dash PR, Whitley GS, Ayling LJ, Johnstone AP, Cartwright JE (2005) Trophoblast apoptosis is
571 inhibited by hepatocyte growth factor through the Akt and beta-catenin mediated up-regulation
572 of inducible nitric oxide synthase. *Cell Signal* 17: 571-580

573

574 Dhakal P, Soares MJ (2017) Single-step PCR-based genetic sex determination of rat tissues and
575 cells. *Biotechniques* 62: 232-233
576
577 Essers MA, Weijzen S, de Vries-Smits AM, Saarloos I, de Ruiter ND, Bos JL, Burgering BM
578 (2004) FOXO transcription factor activation by oxidative stress mediated by the small GTPase
579 Ral and JNK. *EMBO J* 23: 4802–4812
580
581 Ferretti C, Bruni L, Dangles-Marie V, Pecking AP, Bellet D (2007) Molecular circuits shared
582 by placental and cancer cells, and their implications in the proliferative, invasive and migratory
583 capacities of trophoblasts. *Hum Reprod Update* 13: 121-141
584
585 Fiddes RJ, Campbell DH, Janes PW, Sivertsen SP, Sasaki H, Wallasch C, Daly RJ (1998)
586 Analysis of Grb7 recruitment by heregulin-activated erbB receptors reveals a novel target
587 selectivity for erbB3. *J Biol Chem* 273: 7717-7724
588
589 Fisher SJ (2015) Why is placentation abnormal in preeclampsia? *Am J Obstet Gynecol*
590 213(Suppl): S115-S122
591
592 Fock V, Plessl K, Draxler P, Otti GR, Fiala C, Knöfler M, Pollheimer J (2015)
593 Neuregulin-1-mediated ErbB2-ErbB3 signalling protects human trophoblasts against
594 apoptosis to preserve differentiation. *J Cell Sci* 128: 4306-4316
595
596 Fukuoka M, Daitoku H, Hatta M, Matsuzaki H, Umemura S, Fukamizu A (2003) Negative
597 regulation of forkhead transcription factor AFX (Foxo4) by CBP-induced acetylation. *Int J*
598 *Mol Med* 12: 503–508

Gardner RL, Beddington RS (1988) Multi-lineage 'stem' cells in the mammalian embryo. *J Cell Sci Suppl* 10: 11-27

Han BW, Ye H, Wei PP, He B, Han C, Chen ZH, Chen YQ, Wang WT (2018) Global identification and characterization of lncRNAs that control inflammation in malignant cholangiocytes. *BMC Genomics* 19: 735

Harris LK, Smith SD, Keogh RJ, Jones RL, Baker PN, Knöfler M, Cartwright JE, Whitley GS, Aplin JD (2010) Trophoblast- and vascular smooth muscle cell-derived MMP-12 mediates elastolysis during uterine spiral artery remodeling. *Am J Pathol* 177: 2103-2115

Haslinger P, Haider S, Sonderegger S, Otten JV, Pollheimer J, Whitley G, Knöfler M (2013) AKT isoforms 1 and 3 regulate basal and epidermal growth factor-stimulated SGHPL-5 trophoblast cell migration in humans. *Biol Reprod* 88: 54

Hemberger M (2002) The role of the X chromosome in mammalian extra embryonic development. *Cytogenet Genome Res* 99: 210-217

Herman L, Todeschini AL, Veitia RA (2021) Forkhead transcription factors in health and disease. *Trends Genet* 37: 460-475

Hosaka T, Biggs WH 3rd, Tieu D, Boyer AD, Varki NM, Cavenee WK, Arden KC (2004) Disruption of forkhead transcription factor (FOXO) family members in mice reveals their functional diversification. *Proc Natl Acad Sci USA* 101: 2975–2980

Huang C, Santofimia-Castaño P, Iovanna J (2021) NUPR1: a critical regulator of the antioxidant system. *Cancers (Basel)* 13: 3670

Huang D, Sherman B, Lempicki R (2009) Systematic and integrative analysis of large gene lists using DAVID bioinformatics resources. *Nat Protoc* 4: 44–57

Huang H, Tindall DJ (2011) Regulation of FOXO protein stability via ubiquitination and proteasome degradation. *Biochim Biophys Acta* 1813: 1961–1964

Iqbal K, Pierce SH, Kozai K, Dhakal P, Scott RL, Roby KF, Vyhlidal CA, Soares MJ (2021) Evaluation of placentation and the role of the aryl hydrocarbon receptor pathway in a rat model of dioxin exposure. *Environ Health Perspect* 129: 117001.

Iwatsuki K, Oda M, Sun W, Tanaka S, Ogawa T, Shiota K (1998) Molecular cloning and characterization of a new member of the rat placental prolactin (PRL) family, PRL-like protein H. *Endocrinology* 139: 4976-4983

Iwatsuki K, Shinozaki M, Sun W, Yagi S, Tanaka S, Shiota K (2000) A novel secretory protein produced by rat spongiotrophoblast. *Biol Reprod* 62: 1352-1359

John RM (2017) Imprinted genes and the regulation of placental endocrine function: pregnancy and beyond. *Placenta* 56: 86-90

Kamei T, Jones SR, Chapman BM, McGonigle KL, Dai G, Soares MJ (2002) The

649 phosphatidylinositol 3-kinase/Akt signaling pathway modulates the endocrine differentiation
650 of trophoblast cells. *Mol Endocrinol* 16: 1469-1481
651
652 Kaneko T (2017) Genome editing of rat. *Methods Mol Biol* 1630: 101-108.
653
654 Kent LN, Konno T, Soares MJ (2010) Phosphatidylinositol 3 kinase modulation of trophoblast
655 cell differentiation. *BMC Dev Biol* 10: 97
656
657 Kent LN, Ohboshi S, Soares MJ (2012) Akt1 and insulin-like growth factor 2 (Igf2) regulate
658 placentation and fetal/postnatal development. *Int J Dev Biol* 56: 255-261
659
660 Kent LN, Rumi MA, Kubota K, Lee DS, Soares MJ (2011) FOSL1 is integral to establishing
661 the maternal-fetal interface. *Mol Cell Biol* 31: 4801-4813
662
663 Knipp GT, Audus KL, Soares MJ (1999) Nutrient transport across the placenta. *Adv Drug*
664 *Deliv Rev* 38: 41-58
665
666 Knöfler M, Haider S, Saleh L, Pollheimer J, Gamage TKJB, James J (2019) Human placenta
667 and trophoblast development: key molecular mechanisms and model systems. *Cell Mol Life Sci*
668 76: 3479-3496
669
670 Kummer D, Ebnet K (2018) Junctional adhesion molecules (JAMs): the JAM-integrin
671 connection. *Cells* 7: 25
672
673 LaFleur DW, Nardelli B, Tsareva T, Mather D, Feng P, Semenuk M, Taylor K, Buergin M,

674 Chinchilla D, Roshke V, et al. (2001) Interferon-kappa, a novel type I interferon expressed in
675 human keratinocytes. *J Biol Chem* 276: 39765-39771
676
677 Lam EW, Brosens JJ, Gomes AR, Koo CY (2013) Forkhead box proteins: tuning forks for
678 transcriptional harmony. *Nat Rev Cancer* 13: 482-495
679
680 Liu W, Li Y, Luo B (2020) Current perspective on the regulation of FOXO4 and its role in
681 disease progression. *Cell Mol Life Sci* 77: 651-663
682
683 Maltepe E, Fisher SJ (2015) Placenta: the forgotten organ. *Annu Rev Cell Dev Biol* 31:
684 523-552
685
686 Manning BD, Cantley LC (2007) AKT/PKB signaling: navigating downstream. *Cell* 129:
687 1261-1274
688
689 Manning BD, Toker A (2017) AKT/PKB signaling: navigating the network. *Cell* 169: 381-405
690
691 Mashima R, Okuyama T (2015) The role of lipoxygenases in pathophysiology; new insights
692 and future perspectives. *Redox Biol* 6: 297-310
693
694 Morey R, Farah O, Kallol S, Requena DF, Meads M, Moretto-Zita M, Soncin F, Laurent LC,
695 Parast MM (2021) Transcriptomic drivers of differentiation, maturation, and polyploidy in
696 human extravillous trophoblast. *Front Cell Dev Biol* 9: 702046
697
698 Muto M, Chakraborty D, Varberg KM, Moreno-Irusta A, Iqbal K, Scott RL, McNally RP,

699 Choudhury RH, Aplin JD, Okae H, et al. (2021) Intersection of regulatory pathways
700 controlling hemostasis and hemochorial placentation. *Proc Natl Acad Sci USA* 118:
701 e2111267118
702
703 Nirgude S, Choudhary B (2021) Insights into the role of GPX3, a highly efficient plasma
704 antioxidant, in cancer. *Biochem Pharmacol* 184: 114365
705
706 Nteeba J, Varberg KM, Scott RL, Simon ME, Iqbal K, Soares MJ (2020) Poorly controlled
707 diabetes mellitus alters placental structure, efficiency, and plasticity. *BMJ Open Diabetes Res*
708 *Care* 8: e001243
709
710 Pijnenborg R, Robertson WB, Brosens I, Dixon G (1981) Trophoblast invasion and the
711 establishment of haemochorial placentation in man and laboratory animals. *Placenta* 2:
712 71-91
713
714 Pijnenborg R, Vercruysse L (2010) Animal models of deep trophoblast invasion. In *Placental*
715 *Bed Disorders*, Pijnenborg R, Brosens I, Romero R (eds) pp 127-139. Cambridge: Cambridge
716 University Press
717
718 Plaks V, Berkovitz E, Vandoorne K, Berkutzki T, Damari GM, Haffner R, Dekel N, Hemmings
719 BA, Neeman M, Harmelin A (2011) Survival and size are differentially regulated by placental
720 and fetal PKBalpha/AKT1 in mice. *Biol Reprod* 84: 537-545
721
722 Pollheimer J, Knöfler M (2005) Signalling pathways regulating the invasive differentiation of
723 human trophoblasts: a review. *Placenta* 26(Suppl A): S21-S30

Qayyum N, Haseeb M, Kim MS, Choi S (2021) Role of thioredoxin-interacting protein in diseases and its therapeutic outlook. *Int J Mol Sci* 22: 2754

Qiu Q, Yang M, Tsang BK, Gruslin A (2004) Both mitogen-activated protein kinase and phosphatidylinositol 3-kinase signalling are required in epidermal growth factor-induced human trophoblast migration. *Mol Hum Reprod* 10: 677-684

Roberts RM, Green JA, Schulz LC (2016) The evolution of the placenta. *Reproduction* 152: R179-R189

Satapathy S, Wilson MR (2021) The dual roles of clusterin in extracellular and intracellular proteostasis. *Trends Biochem Sci* 46: 652-660

Schmitt-Ney M (2020). The FOXO's advantages of being a family: considerations on function and evolution. *Cells* 9: 787

Sharma N, Kubaczka C, Kaiser S, Nettersheim D, Mughal SS, Riesenberg S, Hölzel M, Winterhager E, Schorle H (2016) Tpbpa-Cre-mediated deletion of TFAP2C leads to deregulation of Cdkn1a, Akt1 and the ERK pathway, causing placental growth arrest. *Development* 143: 787-798

Shukla V, Soares MJ (2022) Modeling trophoblast cell-guided uterine spiral artery transformation in the rat. *Int J Mol Sci* 23: 2947

749 Sies H, Cadenas E (1985) Oxidative stress: damage to intact cells and organs. *Philos Trans R*
750 *Soc Lond B Biol Sci* 311: 617-631
751
752 Soares MJ (2004) The prolactin and growth hormone families: pregnancy-specific
753 hormones/cytokines at the maternal-fetal interface. *Reprod Biol Endocrinol* 2: 51
754
755 Soares MJ, Chakraborty D, Rumi MAK, Konno T, Renaud SJ (2012) Rat placentation: an
756 experimental model for investigating the hemochorial maternal-fetal interface. *Placenta* 33:
757 233-243
758
759 Soares MJ, Chapman BM, Rasmussen CA, Dai G, Kamei T, Orwig KE (1996) Differentiation
760 of trophoblast endocrine cells. *Placenta* 17: 277-289
761
762 Soares MJ, Konno T, Alam SM (2007) The prolactin family: effectors of pregnancy-dependent
763 adaptations. *Trends Endocrinol Metab* 18: 114-121
764
765 Soares MJ, Varberg KM, Iqbal K (2018) Hemochorial placentation: development, function,
766 and adaptations. *Biol Reprod* 99: 196-211
767
768 Takagi N, Sasaki M (1975) Preferential inactivation of the paternally derived X chromosome in
769 the extraembryonic membranes of the mouse. *Nature* 256: 640-642
770
771 van der Horst A, de Vries-Smits AM, Brenkman AB, van Triest MH, van den Broek N, Colland
772 F, Maurice MM, Burgering BM (2006) FOXO4 transcriptional activity is regulated by
773 monoubiquitination and USP7/HAUSP. *Nat Cell Biol* 8: 1064–1073

Varberg KM, Iqbal K, Muto M, Simon ME, Scott RL, Kozai K, Choudhury RH, Aplin JD, Biswell R, Gibson M, *et al.*, (2021) ASCL2 reciprocally controls key trophoblast lineage decisions during hemochorial placenta development. *Proc Natl Acad Sci USA* 118: e2016517118

West JD, Papaioannou VE, Frels WI, Chapman VM (1978) Preferential expression of the maternally derived X chromosome in extraembryonic tissues of the mouse. *Basic Life Sci* 12: 361-377

Wooding P & Burton G (2008) *Comparative Placentation*. Springer-Verlag, Heidelberg, Germany

Yang ZZ, Tschopp O, Hemmings-Mieszczak M, Feng J, Brodbeck D, Perentes E, Hemmings BA (2003) Protein kinase B alpha/Akt1 regulates placental development and fetal growth. *J Biol Chem* 278: 32124-32131

FIGURE LEGENDS

Figure 1. In vivo genome editing of the rat *Akt1* locus. A) Schematic representation of the rat *Akt1* gene (*Akt1*$^{+/+}$) and guide RNA target sites within Exons 4 and 7 (NM_033230.3). Red bars beneath Exons 4 and 7 correspond to the 5' and 3' guide RNAs used in the genome editing. **B)** The mutant *Akt1* allele (*Akt1*$^{-/-}$) possesses a 1,332 bp deletion. Parts of Exons 4 and 7 and all of Exons 5 and 6 are deleted, leading to a frameshift and premature Stop codon in Exon 7. **C)** Amino acid sequences for AKT1$^{+/+}$ and AKT1$^{-/-}$. The red sequence corresponds

to the frameshift in Exon 7. The blue, red, and green highlighted amino acid sequence regions correspond to the pleckstrin homology (**PH**), kinase, and regulatory domains, respectively. **D)** Offspring were backcrossed to wild type rats, and heterozygous mutant rats were intercrossed to generate homozygous mutants. Wild type (+/+), heterozygous (+/-), and homozygous mutant (-/-) genotypes were detected by PCR. **E)** Western blot analysis of AKT1, pan-AKT, phospho (p)-AKT (Ser^{473}) protein in $Akt1^{+/+}$ and $Akt1^{-/-}$ placentas at gd 18.5. GAPDH was used as a loading control.

Figure 2. $Akt1^{-/-}$ placentas and fetuses are growth restricted, and $Akt1^{-/-}$ rats exhibit postnatal growth restriction. Placentas (**A**) and fetuses (**B**) were dissected from $Akt1^{+/-}$ intercrosses at gd 18.5 and weighed; **C**, fetus/placenta ratio. Placentas were then separated into junctional zone (**JZ**; **D**) and labyrinth zone (**LZ**;**E**) compartments, and weighed; **F**, JZ/JZ ratio. Graphs represent means ± SEM. $Akt1^{+/+}$, n = 22 from 6 dams; $Akt1^{-/-}$, n = 17 from 6 dams. Asterisks denote statistical differences (**$P < 0.01$; ***$P < 0.001$) as determined by Student's or Welch's *t*-test. Body weights of $Akt1^{+/+}$ and $Akt1^{-/-}$ pups were measured from two to eight weeks after birth: males **(G)** and females **(H)**. Graphs represent means ± SEM. n = 13-23/group. Asterisks denote statistical differences (*$P < 0.05$; ***$P < 0.001$) as determined by Student's or Welch's *t*-test. **I**) Vimentin immunostaining of gd 18.5 $Akt1^{+/+}$ and $Akt1^{-/-}$ placentation sites. The junctional zone (**JZ**) is negative for vimentin immunostaining, whereas the uterine-placental interface (**UPI**) and labyrinth zone (**LZ**) stain positive for vimentin. Scale bars=1000 μm

Figure 3. AKT1 deficiency alters the transcriptomes of the junctional zone. A) Heat maps depicting differentially expressed genes between $Akt1^{+/+}$ and $Akt1^{-/-}$ junctional zones. The heatmap color keys represent z-scores of TPM values. **B**) RT-qPCR validation of RNA-seq

results (n=6/group). Graphs represent means ± SEM. Asterisks denote statistical difference (*P<0.05; **P<0.01; ***P<0.001) as determined by Student's or Welch's t-test.

Figure 4. FOXO4 is a target of PI3K/AKT signaling. A) Expressions of transcripts for several FOX transcription factors in the junctional zone. **B**) In situ localization of transcripts for *Foxo4* with *Prl7b1* (invasive trophoblast-specific transcript) in the placentation site at gd 18.5 of rat pregnancy. Scale bars = 1000 μm. **C**) RT-qPCR measurements of *Foxo4* transcripts in the uterine-placental interface, junctional and labyrinth zones during the second half of gestation (n = 6-9/group). Graphs represent means ± SEM. Asterisks denote statistical difference (**P < 0.01) as determined by Steel test. UPI: uterine-placental interface; JZ: junctional zone; and LZ: labyrinth zone. **D**) Western blot analysis of phospho (p)-FOXO4 (Ser^{262}) and FOXO4 proteins in $Akt1^{+/+}$ and $Akt1^{-/-}$ placentas at gd 18.5. GAPDH was used as a loading control. **E)** RT-qPCR measurements of *Foxo4* transcripts in the stem state and following induction of differentiation (n = 4-6/group). Graphs represent means ± SEM. Asterisks denote statistical difference (vs Stem, *P < 0.05) as determined by Dunnett's test. Western blot analysis of phospho (p)-FOXO4 (Ser^{262}), FOXO4, p-AKT (Ser^{473}), and pan-AKT proteins in the stem and differentiating (day 15 of differentiation, D15) states **(F)**, and in the differentiating state (D15) following treated with vehicle (0.1% DMSO) or a phosphatidylinositol 3-kinase (**PI3K**) inhibitor (LY294002, 10 μM) for 1 h **(G)**. GAPDH was used as a loading control.

Figure 5. In vivo genome editing of the rat *Foxo4* locus. A) Schematic representation of the rat *Foxo4* gene ($Foxo4^{Xm+}$) and guide RNA target sites within Exons 2 and 3 (NM_001106943.1). Red bars beneath Exons 2 and 3 correspond to the 5' and 3' guide RNAs used in the genome editing. **B)** The mutant *Foxo4* allele ($Foxo4^{Xm-}$) possesses a 3,096 bp

deletion. Parts of Exons 2 and 3 are deleted, leading to a frameshift and premature Stop codon in Exon 3. **C)** Amino acid sequences for FOXO4^{Xm+} and FOXO4^{Xm-}. The red sequence corresponds to the frameshift in Exon 3. The green, red, dark blue, and light blue highlighted amino acid sequence regions correspond to the forkhead winged-helix DNA-binding domain (**FHD**), nuclear localization sequence (**NLS**), nuclear export sequence (**NES**), and transactivation domain (**TAD**), respectively. **D)** Heterozygous mutant female rats were crossed to wild type male rats to generate hemizygous null male rats. Wild type (+/+), heterozygous (+/-), and hemizygous null (-/y) genotypes were detected by PCR. **E)** Western blot analysis of FOXO4 protein in the junctional zone of *Foxo4*$^{Xm+}$ ($X^{m+}Y$ and $X^{m+}X^{p+}$) and *Foxo4*$^{Xm-}$ ($X^{m-}Y$ and $X^{m-}X^{p+}$) placentas at gd 18.5. GAPDH was used as a loading control.

Figure 6. *Foxo4* hemizygous null and *Foxo4* maternally inherited heterozygous conceptuses exhibit placental overgrowth, and FOXO4 deficiency alters the transcriptomes of the junctional zone. Placentas **(A)** and fetuses **(B)** were dissected from *Foxo4* heterozygous females mated with wild type males at gd 18.5 and weighed; **C**) fetus/placenta ratio. Placentas were then separated into junctional zone (**JZ, D**) and labyrinth zone (**LZ, E**) compartments, and weighed; **F**, JZ/LZ weight ratio. Graphs represent means ± SEM. $X^{m+}Y$, n = 25; $X^{m-}Y$, n = 31; $X^{m+}X^{p+}$, n = 14; $X^{m-}X^{p+}$, n = 22 from 8 dams. Asterisks denote statistical differences (***$P < 0.001$) as determined by Student's or Welch's *t*-test. **G**) Vimentin immunostaining of gd 18.5 *Foxo4*$^{Xm+}$ and *Foxo4*^{Xm} placentation sites. The junctional zone (**JZ**) is negative for vimentin immunostaining, whereas the uterine-placental interface (**UPI**) and labyrinth zone (**LZ**) stain positive for vimentin. Scale bars=1000 μm. **H**) Heat maps depicting differentially expressed genes in *Foxo4*$^{Xm+}$ versus *Foxo4*$^{Xm-}$junctional zones. The heatmap color keys represent z-scores of TPM values. **I**) RT-qPCR validation of RNA-seq results (n=6/group). Graphs represent means ± SEM. Asterisks denote statistical

difference (**P<0.01; ***P<0.001) as determined by Student's or Welch's t-test.

Figure 7. Reciprocal relationship between AKT1 and FOXO4 in the junctional zone. Venn diagram and heatmaps representing overlap of differentially expressed genes inversely regulated by AKT1 and FOXO4. The heatmap color keys represent z-scores of TPM values.

Figure 8. FOXO4 alters the rat TS cell. FOXO4 knockdown efficiency was validated by RT-qPCR (**A**, n = 4/group) or western blot **(B)** analyses in rat TS cells at day 15 of differentiation following transduction with lentivirus containing a control shRNA or one of two independent *Foxo4*-specific shRNAs. Graphs represent means ± SEM. Asterisks denote statistical difference (vs Control shRNA, $*P < 0.05$) as determined by Student's or Welch's *t*-test. **C)** Heatmap depicting differentially expressed genes between control and *Foxo4* shRNA-treated rat TS cells. **D)** RT-qPCR validation of RNA-seq results (Control shRNA, n = 4; *Foxo4* shRNA 1, n = 4; *Foxo4* shRNA 2, n = 4). Graphs represent means ± SEM. Asterisks denote statistical difference (compared to Control shRNA, $*P < 0.05$; $**P < 0.01$; $***P < 0.001$) as determined by Student's or Welch's *t*-test.

Figure 1

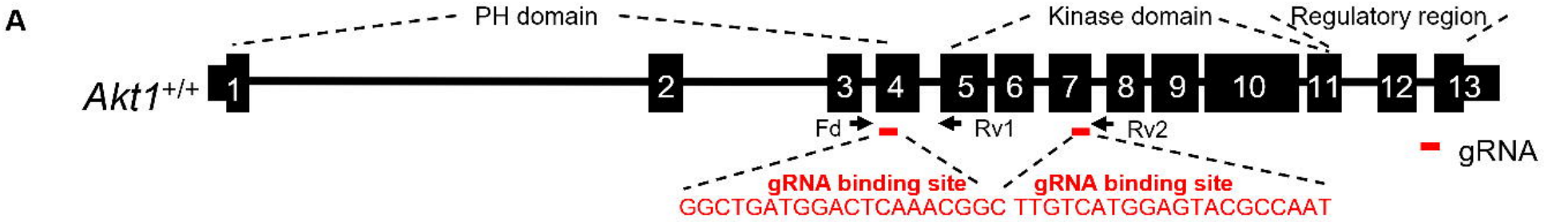

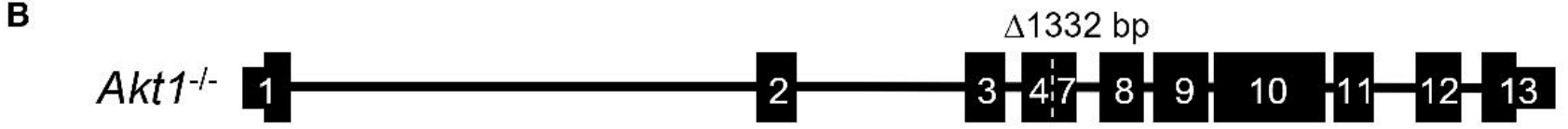

C

AKT1$^{+/+}$

MNDVAIVKEGWLHKRGEYIKTWRPRYFLLKNDGTFIGYKERP
QDVEQRESPLNNFSVAQCQLMKTERPRPNTFIIRCLQWTTVIE
RTFHVETPEEREEWTTAIQTVADGLKRQEEETMDFRSGSPSD
NSGAEEMEVALAKPKHRVTMNEFEYLKLLGKGTFGKVILVKEK
ATGRYYAMKILKKEVIVAKDEVAHTLTENRVLQNSRHPFLTAL
KYSFQTHDRLCFVMEYANGGELFFHLSRERVFSEDRARFYGA
EIVSALDYLHSEKNVVYRDLKLENLMLDKDGHIKITDFGLCKEG
IKDGATMKTFCGTPEYLAPEVLEDNDYGRAVDWWGLGVVMY
EMMCGRLPFYNQDHEKLFELILMEEIRFPRTLGPEAKSLLSGL
LKKDPTQRLGGGSEDAKEIMQHRFFANIVWQDVYEKKLSPPF
KPQVTSETDTRYFDEEFTAQMITITPPDQDDSMECVDSERRP
HFPQFSYSASGTA

AKT1$^{-/-}$

MNDVAIVKEGWLHKRGEYIKTWRPRYFLLKNDGTFIGYKERP
QDVEQRESPLNNFSVAQCQLMKTERPRPNTFIIRCLQWTTVIE
RTFHVETPEEREEWTTAIQTVADGLKQWGRALLPPVS Stop

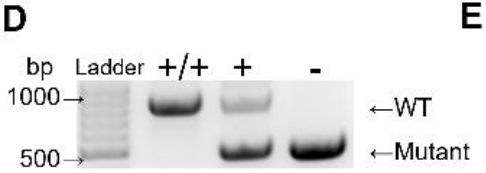

PH domain
Kinase domain
Regulatory region

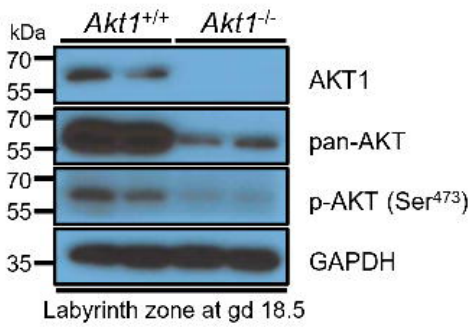

Figure 2

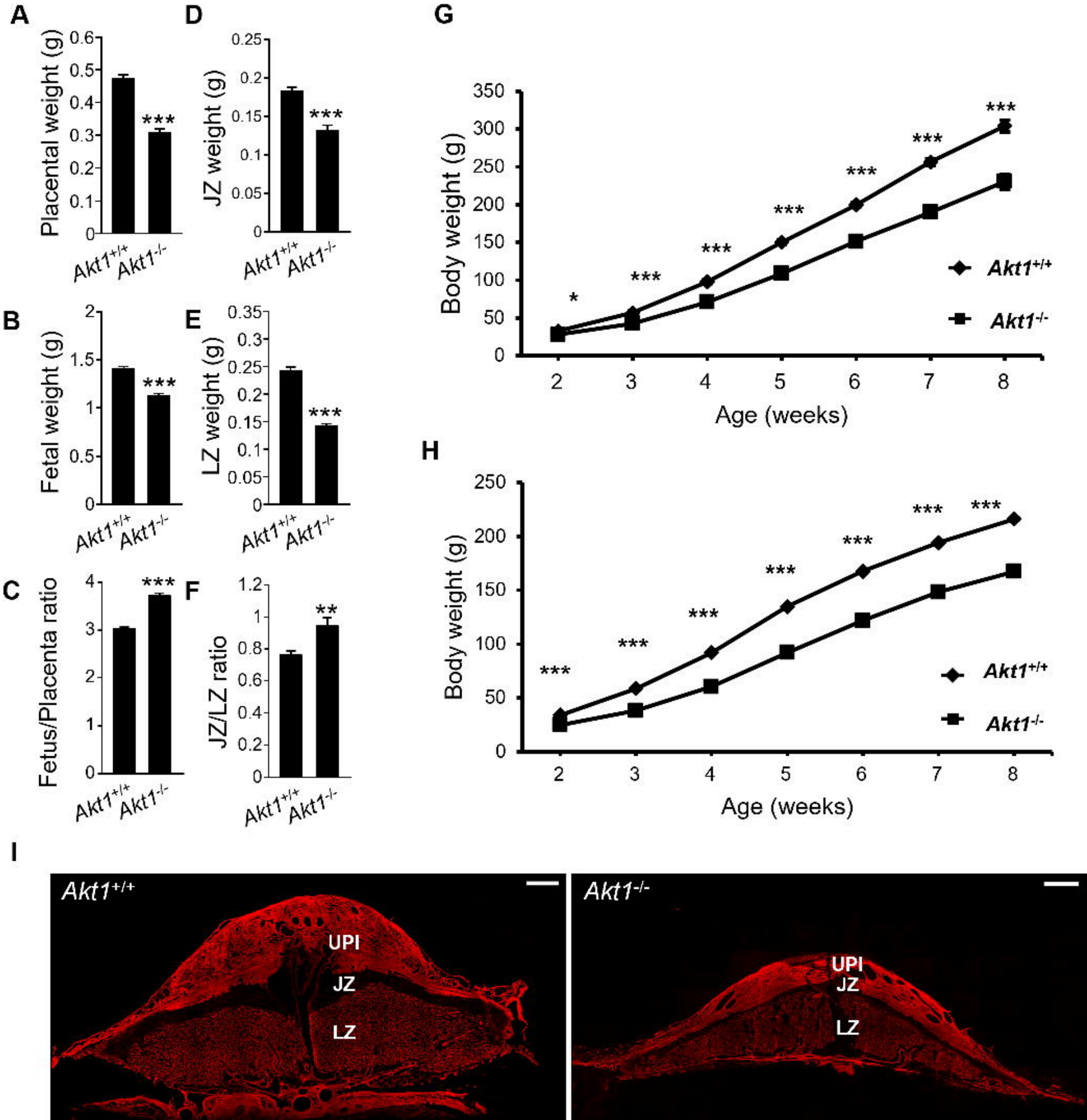
A
Placental weight (g)
0.6
0.5
0.4
0.3
0.2
0.1
0
***
Akt1+/+
Akt1-/-
D
JZ weight (g)
0.25
0.2
0.15
0.1
0.05
0
***
Akt1+/+
Akt1-/-
B
Fetal weight (g)
2
1.5
1
0.5
0
***
Akt1+/+
Akt1-/-
E
LZ weight (g)
0.35
0.3
0.25
0.2
0.15
0.1
0.05
0
***
Akt1+/+
Akt1-/-
C
Fetus/Placenta ratio
4
3
2
1
0
***
Akt1+/+
Akt1-/-
F
JZ/LZ ratio
1.2
1
0.8
0.6
0.4
0.2
0
**
Akt1+/+
Akt1-/-
G
Body weight (g)
350
300
250
200
150
100
50
0
*
***
***
***
***
***
2
3
4
5
6
7
8
Age (weeks)
Akt1+/+
Akt1-/-
H
Body weight (g)
250
200
150
100
50
0
***
***
***
***
***
***
2
3
4
5
6
7
8
Age (weeks)
Akt1+/+
Akt1-/-
I
Akt1+/+
UPI
JZ
LZ
Akt1-/-
UPI
JZ
LZ

Figure 3

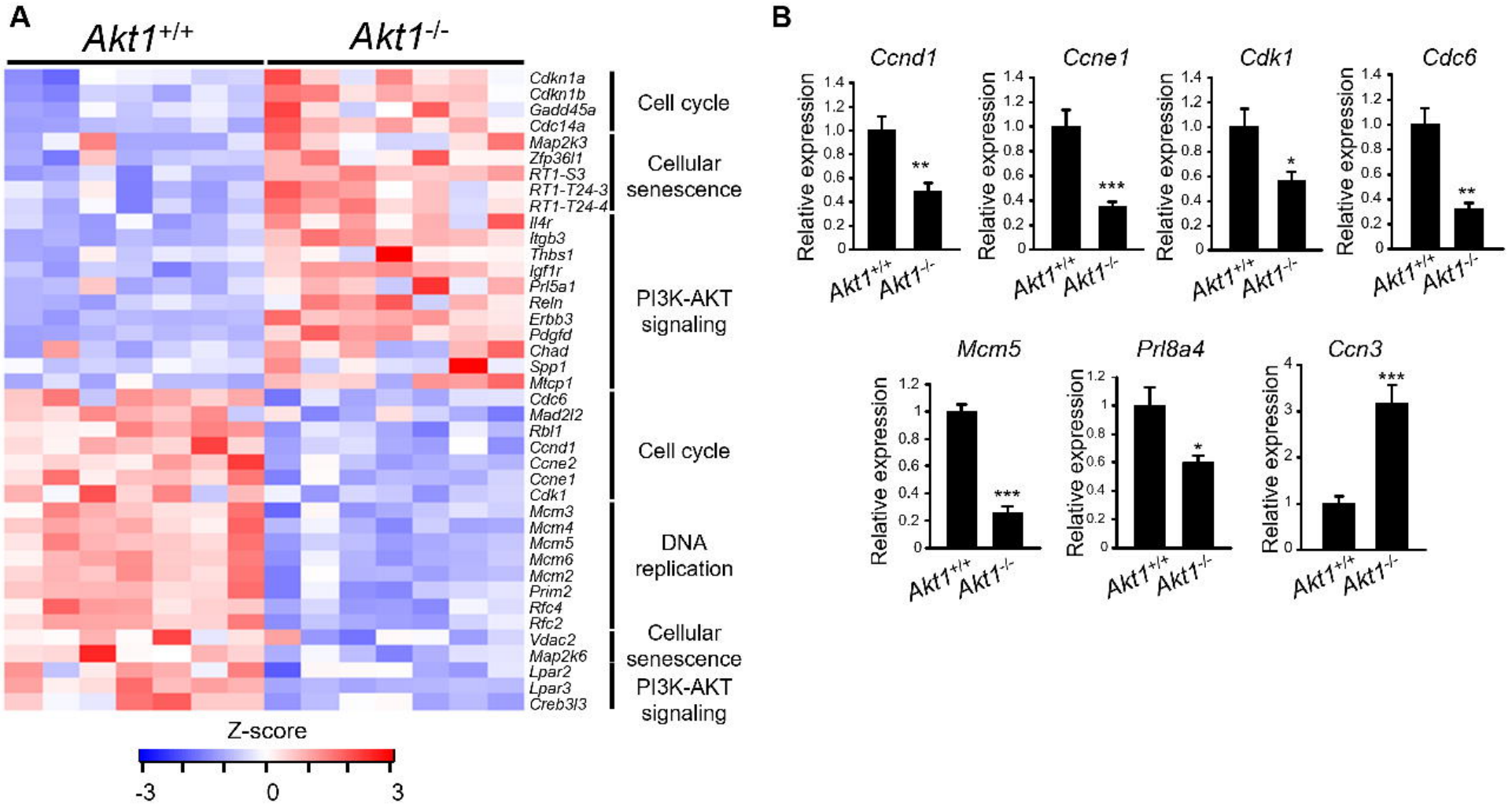
A
Akt1+/+
Akt1-/-
Cdkn1a
Cdkn1b
Gadd45a
Cdc14a
Map2k3
Zfp36l1
RT1-S3
RT1-T24-3
RT1-T24-4
Il4r
Itgb3
Thbs1
Igf1r
Prl5a1
Reln
Erbb3
Pdgfd
Chad
Spp1
Mtcp1
Cdc6
Mad2l2
Rbl1
Ccnd1
Ccne2
Ccne1
Cdk1
Mcm3
Mcm4
Mcm5
Mcm6
Mcm2
Prim2
Rfc4
Rfc2
Vdac2
Map2k6
Lpar2
Lpar3
Creb3l3
Cell cycle
Cellular senescence
PI3K-AKT signaling
Cell cycle
DNA replication
Cellular senescence
PI3K-AKT signaling
Z-score
-3
0
3
B
Ccnd1
Ccne1
Cdk1
Cdc6
Mcm5
Prl8a4
Ccn3
Relative expression
Akt1+/+
Akt1-/-

Figure 4

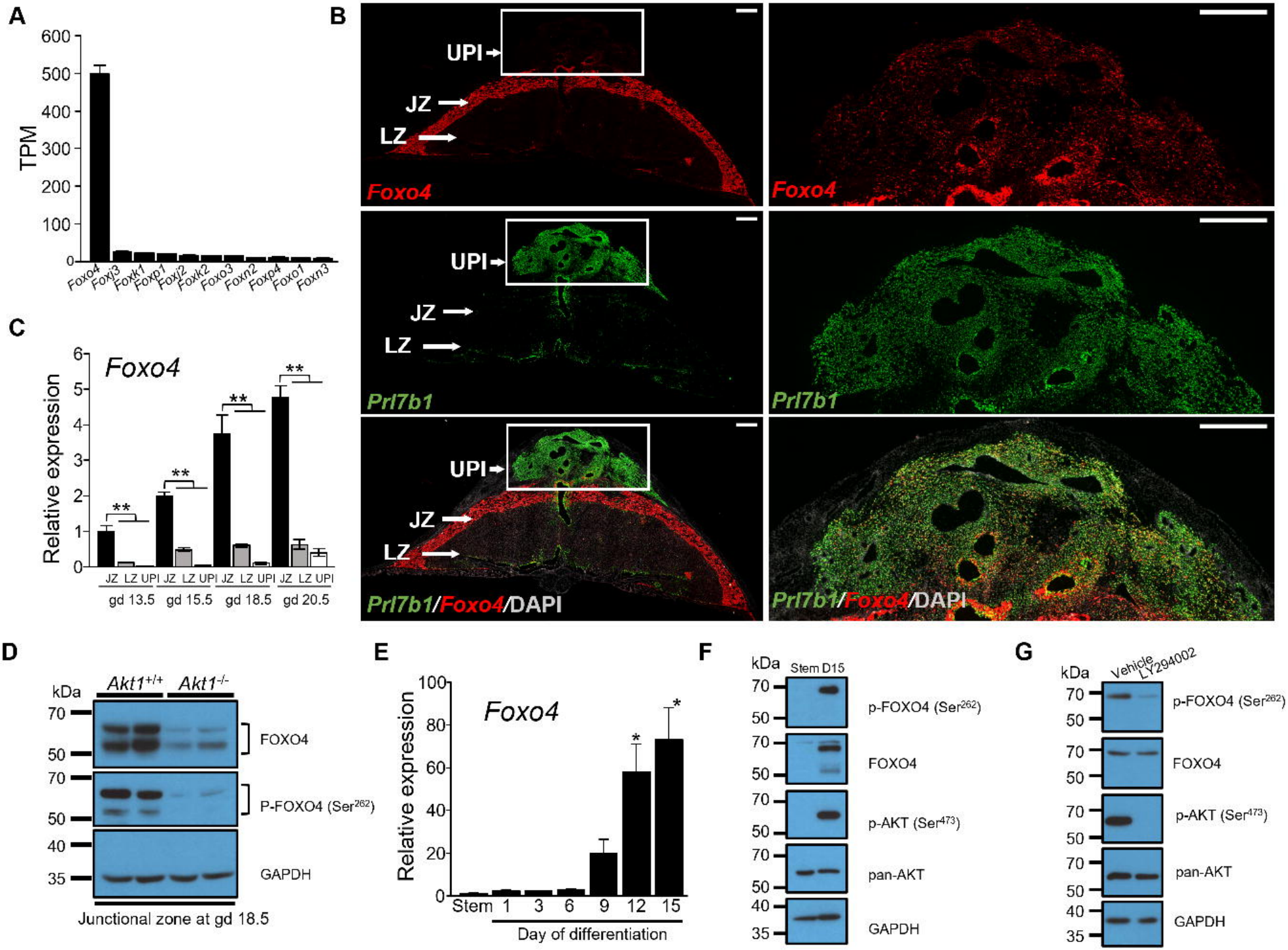
A
TPM
600
500
400
300
200
100
0
Foxo4
Foxi3
Foxk1
Foxp1
Foxi2
Foxk2
Foxo3
Foxn2
Foxp4
Foxo1
Foxn3
B
UPI
JZ
LZ
Foxo4
Foxo4
Prl7b1
Prl7b1
Prl7b1/Foxo4/DAPI
Prl7b1/Foxo4/DAPI
C
Foxo4
Relative expression
**
JZ LZ UPI JZ LZ UPI JZ LZ UPI JZ LZ UPI
gd 13.5
gd 15.5
gd 18.5
gd 20.5
D
kDa
Akt1+/+
Akt1-/-
70
50
70
50
40
35
FOXO4
P-FOXO4 (Ser262)
GAPDH
Junctional zone at gd 18.5
E
Foxo4
Relative expression
100
80
60
40
20
0
*
Stem 1 3 6 9 12 15
Day of differentiation
F
kDa
Stem D15
70
50
p-FOXO4 (Ser262)
FOXO4
p-AKT (Ser473)
pan-AKT
GAPDH
40
35
G
kDa
Vehicle
LY294002
p-FOXO4 (Ser262)
FOXO4
p-AKT (Ser473)
pan-AKT
GAPDH

Figure 5

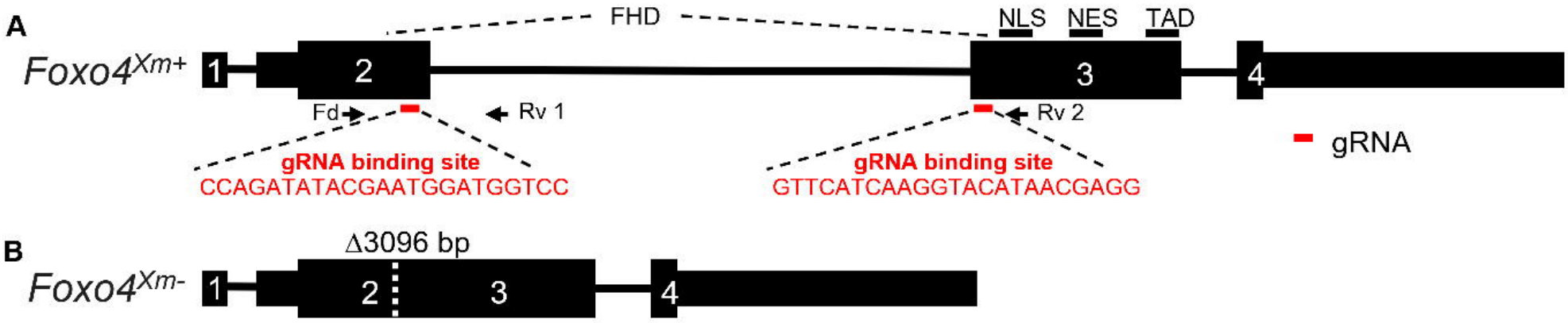

C

FOXO4^{Xm+}

MEPENKKSATEAAAIIDLDPDFEPQSRPRSCTWPLPRPELATE
PPEPSEVEPSLGQKVPTEGHSEPTLLPSRLPEPAGGPQPEILG
AVTGPRKGGSRRNAWGNQSYAELISQAIESAPEKRLTLAQIYE
WMVRTVPYFKDKGDSNSSAGWKNSIRHNLSLHSKFIKVHNEA
TGKSSWWMLNPDGGKGGKAPRRRAASMDSSSKLLRGRSKG
PKKKPSVLPAPPEGATPRSPLGHFAKWSSSPCPRNREEADV
WTTFRPRSSSNASTVSTRLSPMRPESEVLAEEEMPASASSYA
GGVPPTLSEDLELLDGLNLASPHSLLSRSNLSSFSLQHPGLAG
PLHSYGASLFGPIDGSLSAGEGCFSSSQSLEALLTSDTPPPPA
DVLMTQVDPILSQAPTLLLLGGMPSSSKLATGVSLCPTPLEGP
GPSNLVPTLSVMAPPPVMPGAPIPKVLGTPVLASPTEDFSHDR
MPQDLDLDMYMENLECDMDNIISDLMDGEGLDFNFEPDP

FOXO4^{Xm-}

MEPENKKSATEAAAIIDLDPDFEPQSRPRSCTWPLPRPELATE
PPEPSEVEPSLGQKVPTEGHSEPTLLPSRLPEPAGGPQPEILG
AVTGPRKGGSRRNAWGNQSYAELISQAIESAPEKRLTLAQRP
PARALGGC

FHD
NLS
NES
TAD

D

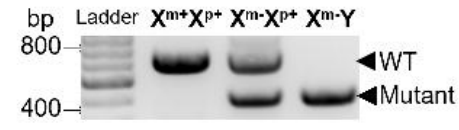

E

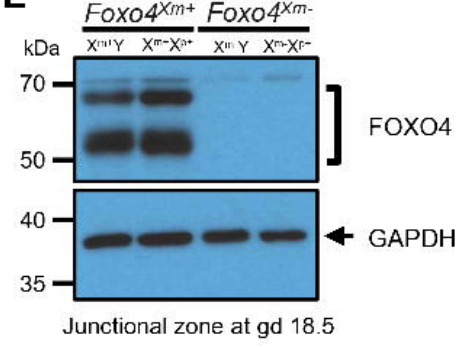

Figure 6

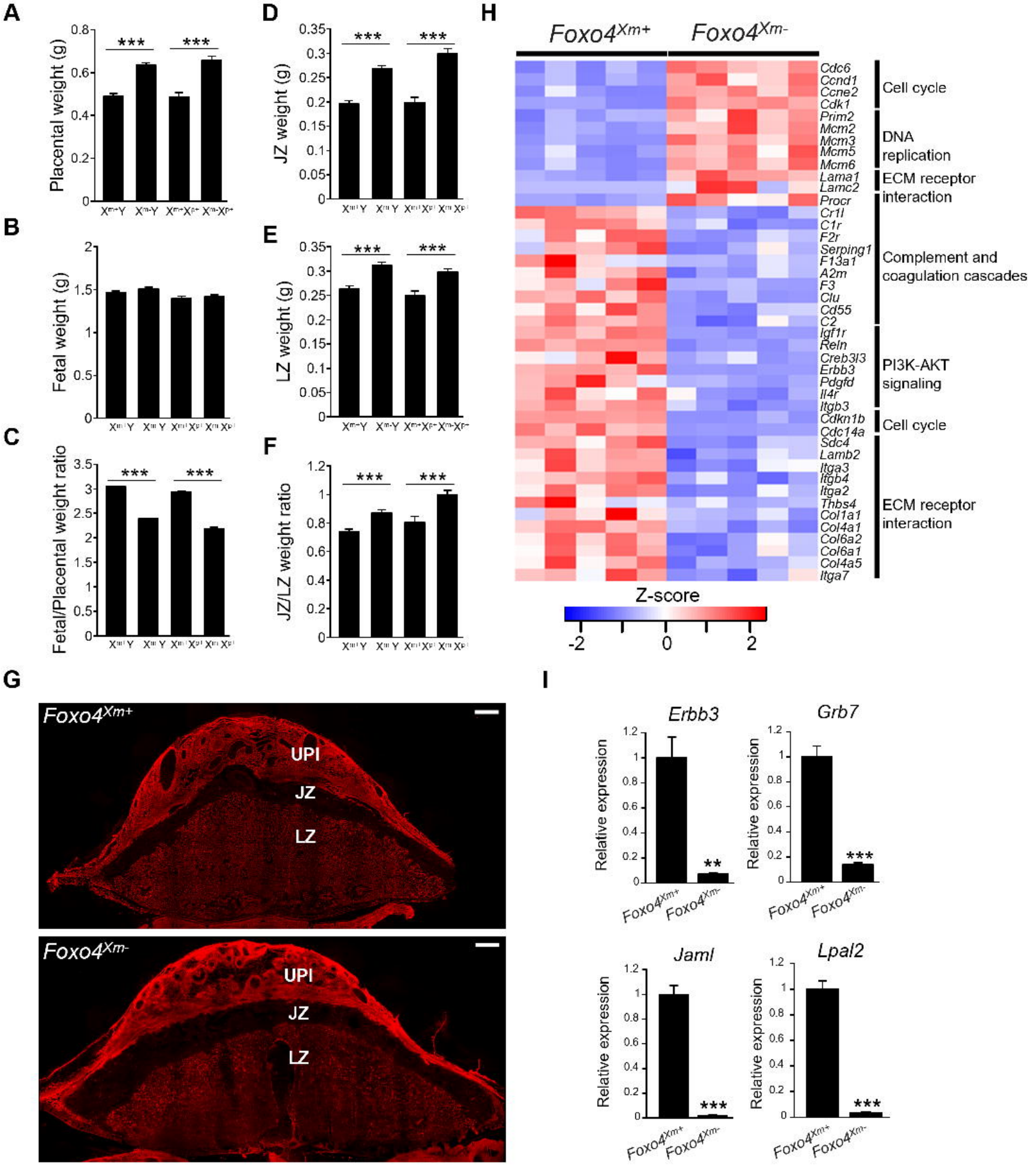
A
Placental weight (g)
B
Fetal weight (g)
C
Fetal/Placental weight ratio
D
JZ weight (g)
E
LZ weight (g)
F
JZ/LZ weight ratio
***
H
Foxo4Xm+
Foxo4Xm-
Cdc6
Ccnd1
Ccne2
Cdk1
Prim2
Mcm2
Mcm3
Mcm5
Mcm6
Lama1
Lamc2
Procr
Cr1l
C1r
F2r
Serping1
F13a1
A2m
F3
Clu
Cd55
C2
Igf1r
Reln
Creb3l3
Erbb3
Pdgfd
Il4r
Itgb3
Cdkn1b
Cdc14a
Sdc4
Lamb2
Itga3
Itgb4
Itga2
Thbs4
Col1a1
Col4a1
Col6a2
Col6a1
Col4a5
Itga7
Cell cycle
DNA replication
ECM receptor interaction
Complement and coagulation cascades
PI3K-AKT signaling
Cell cycle
ECM receptor interaction
Z-score
-2
0
2
G
Foxo4Xm+
Foxo4Xm-
UPI
JZ
LZ
I
Erbb3
Grb7
Jaml
Lpal2
Relative expression
**
***

Figure 7

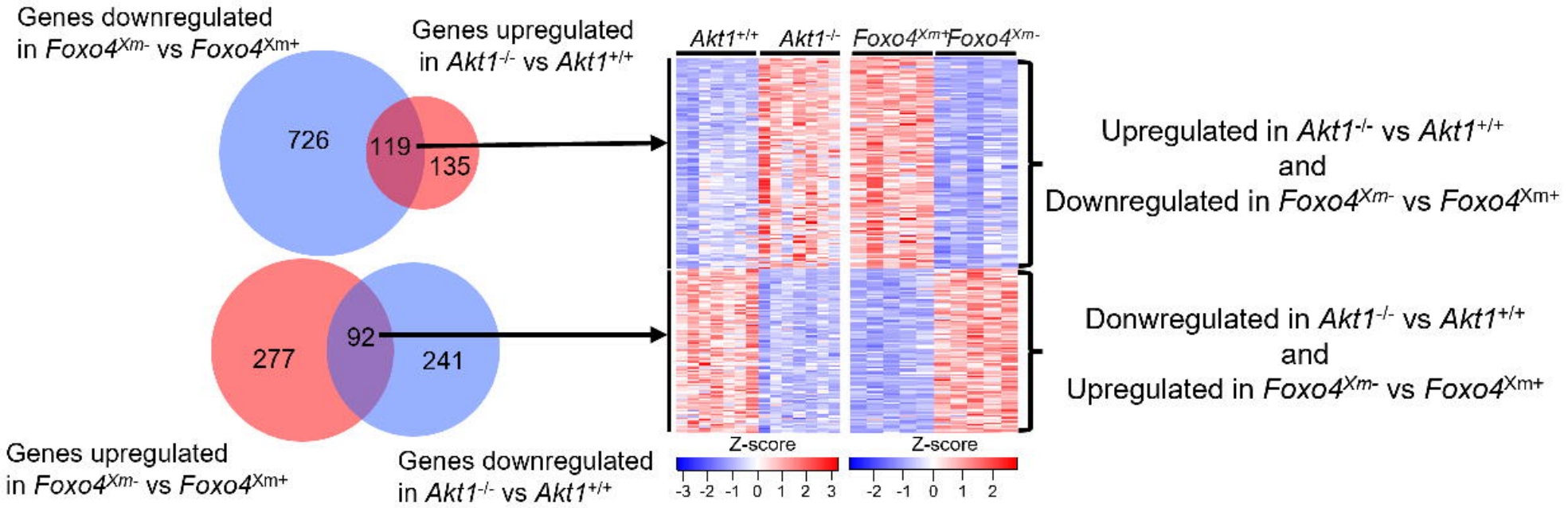
Genes downregulated in Foxo4Xm- vs Foxo4Xm+
Genes upregulated in Akt1-/- vs Akt1+/+
726
119
135
277
92
241
Genes upregulated in Foxo4Xm- vs Foxo4Xm+
Genes downregulated in Akt1-/- vs Akt1+/+
Akt1+/+
Akt1-/-
Foxo4Xm+
Foxo4Xm-
Z-score
-3 -2 -1 0 1 2 3
Z-score
-2 -1 0 1 2
Upregulated in Akt1-/- vs Akt1+/+ and Downregulated in Foxo4Xm- vs Foxo4Xm+
Donwregulated in Akt1-/- vs Akt1+/+ and Upregulated in Foxo4Xm- vs Foxo4Xm+

Figure 8

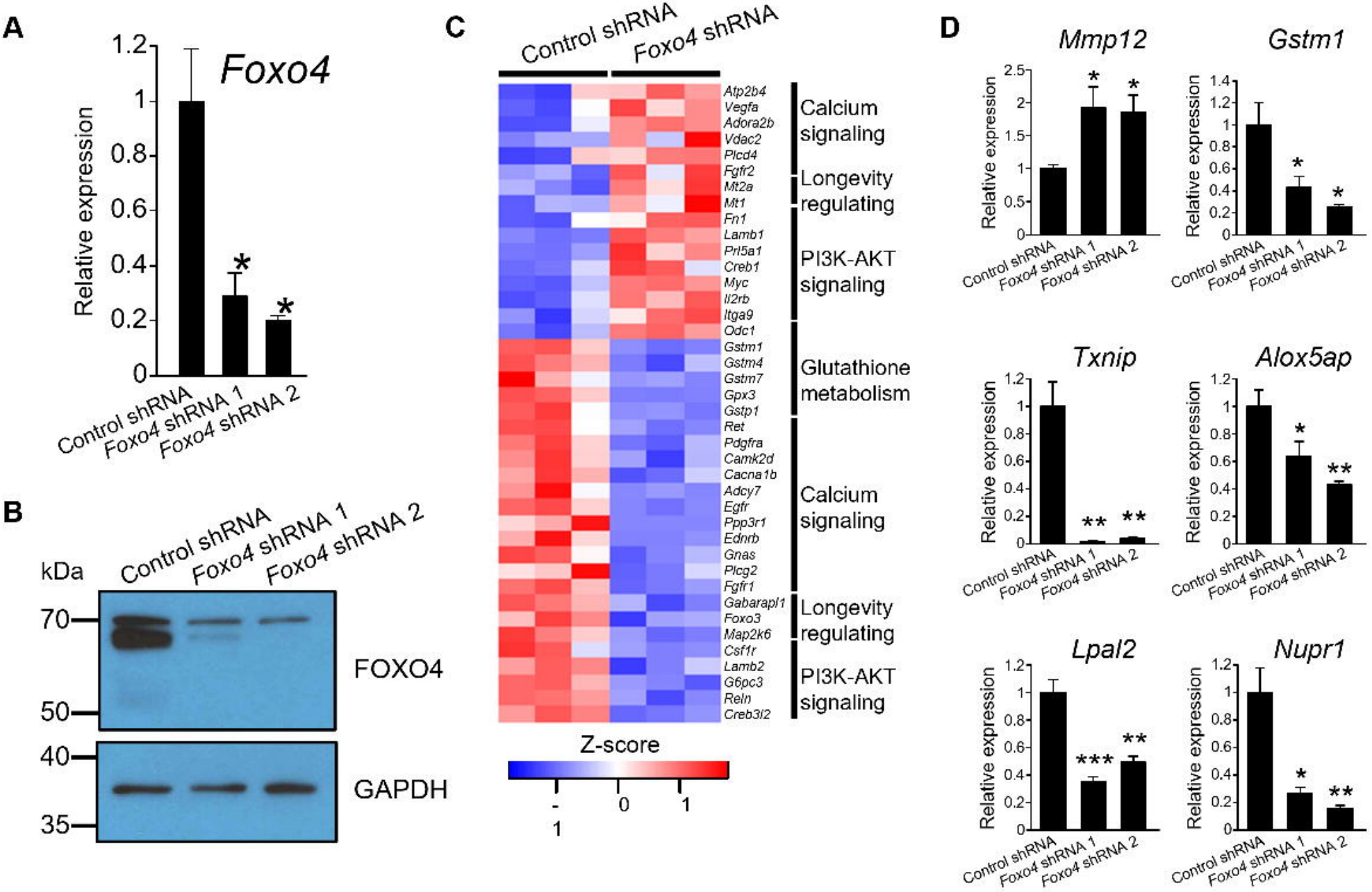
A
Foxo4
Relative expression
1.2
1
0.8
0.6
0.4
0.2
0
*
*
Control shRNA
Foxo4 shRNA 1
Foxo4 shRNA 2
B
kDa
Control shRNA
Foxo4 shRNA 1
Foxo4 shRNA 2
70
50
40
35
FOXO4
GAPDH
C
Control shRNA
Foxo4 shRNA
Atp2b4
Vegfa
Adora2b
Vdac2
Plcd4
Fgfr2
Mt2a
Mt1
Fn1
Lamb1
Prl5a1
Creb1
Myc
Il2rb
Itga9
Odc1
Gstm1
Gstm4
Gstm7
Gpx3
Gstp1
Ret
Pdgfra
Camk2d
Cacna1b
Adcy7
Egfr
Ppp3r1
Ednrb
Gnas
Plcg2
Fgfr1
Gabarapl1
Foxo3
Map2k6
Csf1r
Lamb2
G6pc3
Reln
Creb3l2
Calcium signaling
Longevity regulating
PI3K-AKT signaling
Glutathione metabolism
Calcium signaling
Longevity regulating
PI3K-AKT signaling
Z-score
-1
0
1
D
Mmp12
Gstm1
Txnip
Alox5ap
Lpal2
Nupr1
Relative expression
Control shRNA
Foxo4 shRNA 1
Foxo4 shRNA 2